Plant Physiology®

Sheet-like clay nanoparticles deliver RNA into developing pollen to efficiently silence a target gene

Jiaxi Yong ⓘ ,[1] Run Zhang ⓘ ,[1] Shengnan Bi ⓘ ,[2] Peng Li ⓘ ,[1] Luyao Sun ⓘ ,[1] Neena Mitter,[3] Bernard J. Carroll ⓘ [2,†] and Zhi Ping Xu ⓘ [1,*,†]

1 Australian Institute for Bioengineering and Nanotechnology, The University of Queensland, Brisbane, QLD 4072, Australia
2 School of Chemistry and Molecular Biosciences, The University of Queensland, Brisbane, QLD 4072, Australia
3 Queensland Alliance for Agriculture and Food Innovation, The University of Queensland, Brisbane, QLD 4072, Australia

*Author for communication: gordonxu@uq.edu.au
†Senior authors.
R.Z., B.C., and Z.P.X.: supervised the study; J.Y.: performed the experiments and data analysis and wrote the first draft; S.B.: prepared dsRNA and helped in qPCR experiment; L.S.: performed TEM analysis and prepared some nanoparticles; P.L. and N.M.: prepared dsRNA; J.Y., R.Z., B.C., and Z.P.X.: wrote and revised the manuscript. All authors read and commented on the manuscript. B.C. and Z.P.X. designed the research.
The author responsible for distribution of materials integral to the findings presented in this article in accordance with the policy described in the Instructions for Authors (https://academic.oup.com/plphys/pages/general-instructions) is: Zhi Ping Xu (gordonxu@uq.edu.au).

Abstract

Topical application of double-stranded RNA (dsRNA) can induce RNA interference (RNAi) and modify traits in plants without genetic modification. However, delivering dsRNA into plant cells remains challenging. Using developing tomato (Solanum lycopersicum) pollen as a model plant cell system, we demonstrate that layered double hydroxide (LDH) nanoparticles up to 50 nm in diameter are readily internalized, particularly by early bicellular pollen, in both energy-dependent and energy-independent manners and without physical or chemical aids. More importantly, these LDH nanoparticles efficiently deliver dsRNA into tomato pollen within 2–4 h of incubation, resulting in an 89% decrease in transgene reporter mRNA levels in early bicellular pollen 3-d post-treatment, compared with a 37% decrease induced by the same dose of naked dsRNA. The target gene silencing is dependent on the LDH particle size, the dsRNA dose, the LDH–dsRNA complexing ratio, and the treatment time. Our findings indicate that LDH nanoparticles are an effective nonviral vector for the effective delivery of dsRNA and other biomolecules into plant cells.

Introduction

Bioengineering of plants is now playing a crucial role in addressing the world's growing demand for food and energy (Sadeghi et al., 2017), and is a powerful tool in plant science research. Plants are also attractive bioreactors for the large-scale production of pharmaceuticals (Fischer et al., 2004). In recent decades, genetic modification has been used to manipulate plant physiology and produce commercially beneficial traits in plants (Koch and Kogel, 2014; Altpeter et al., 2016; Cunningham et al., 2018). In particular, transgenes expressing double-stranded RNA (dsRNA) have been effective in conferring resistance to viruses and pests, and in manipulating metabolic pathways in plants (Koch and Kogel, 2014). For research purposes, genetically modified plant viruses have also been used to deliver RNA, induce RNAi, and thereby modify traits in plants. However, the efficacy of genetic engineering and virus-facilitated trait modification varies greatly between different plant species. Moreover, genetically modified varieties may take over a decade to develop to the commercialization stage, and there are

considerable consumer concerns regarding the genetic engineering of crops (Bates, 1995; Key et al., 2008; Cunningham et al., 2018; Liu et al., 2019).

In the recent decade, many nanoparticles have been developed to mediate the delivery of biomolecules into plants, with some demonstrating potential. These include DNA nanostructures (Zhang et al., 2019), mesoporous silica nanoparticles (Martin-Ortigosa et al., 2014), polymer nanoparticles (Jiang et al., 2014), and carbon nanotubes. More specifically, single-walled carbon nanotubes can deliver plasmids (Demirer et al., 2019; Kwak et al., 2019) and siRNAs (Demirer et al., 2020) into leaves via infiltration. Nanoparticle delivery platforms have particular advantages, such as low toxicity, high delivery efficiency, species independence, and subcellular targeting, when applied to plants with minimal or no physical or chemical aids (Lv et al., 2020). However, despite the potential, there have been very few reports of nanoparticle-mediated delivery of functional biomolecules directly into intact plant cells.

LDH is a family of bio-compatible and degradable clay materials, exemplified by naturally existing hydrotalcite, with the general formula of $[M_{1?}\text{-}x^{II}M^{III}_x(OH)_2]^{x+}A^{m?}_{x/m}\cdot nH_2O$, where M^{II} is divalent metal, M^{III} a trivalent metal, and A^{m-} intercalated anions, such as NO_3^- or Cl^- in the precursor salts. LDH has been widely examined for applications in disease diagnosis (Li et al., 2017), cancer therapy (Chen et al., 2018b), and drug/gene delivery in mammalian systems (Xu et al., 2006b; Chen et al., 2018a). The plate-like LDH nanoparticles consist of mixed divalent/trivalent metal hydroxide layers, which are bonded together with anions and water molecules between them. The layered structure and positively charged hydroxide layers make LDH nanoparticles a suitable carrier to deliver negatively charged biomolecules such as DNA, RNA, and proteins (Xu et al., 2007; Zhang et al., 2021). Interestingly, a previous study demonstrated that LDH nanoparticles up to 120 nm in diameter and 5- to 10-nm thick successfully delivered dsRNA as a spray and protected the plant from viral infection (Mitter et al., 2017). In this case, LDH protected the dsRNA from degradation on the leaf surface, allowing the slow release of dsRNA and sustained protection against the virus for at least 20 d after spraying. Smaller delaminated layered double hydroxide (LDH) nanosheets (30 nm in diameter and 0.5- to 2-nm thick, monolayer or bilayer) were reported to enter BY-2 cultured tobacco (Nicotiana tabacum) cells and Arabidopsis thaliana roots (Bao et al., 2016). It is well known that LDH nanosheets are quickly degraded under low pH conditions. The plant apoplast has a lower pH of around 5–5.5 (Kurkdjian and Guern, 1989; Oh et al., 2009; Martiniere et al., 2018), suggesting that LDH nanosheets would be rapidly degraded if not efficiently taken up by plant cells. However, these reports have not clearly demonstrated that unmodified LDH nanoparticles can be internalized by intact plant cells

to deliver functional biomolecules, but given the potential, this possibility warrants further investigation.

During male reproductive development in flowering plants, the microspore mother cell undergoes meiosis to produce four microspores. In tomato (Solanum lycopersicum), each microspore (also referred to as monocellular pollen) undergoes a single round of mitosis to form mature bicellular pollen composed of the generative cell enclosed within the vegetative cell (Polowick and Sawhney, 1993a, 1993b). Studies have reported successful transformation of pollen grains with the help of magnetofection, biolistic gun, and carbon nanotubes (Wang and Jiang, 2011; Zhao et al., 2017; Lew et al., 2020). However, there is no report about applying nanoparticles for direct delivery of dsRNA to pollen to initiate RNA interference. To this end, tomato pollen was chosen as a simple intact plant cell model to investigate the capacity of LDH nanoparticles to facilitate the uptake of dsRNA and the induction of RNAi.

Therefore, this research aimed to (1) determine whether developing tomato pollen internalizes LDH nanoparticles, and if so, to find the size exclusion limit for the nanoparticles; (2) reveal whether LDH nanoparticles facilitate the dsRNA delivery to tomato pollen in comparison with naked dsRNA; and (3) evaluate how efficiently LDH nanoparticles deliver functional dsRNA into developing pollen to trigger RNAi and silence a target gene. In this research, we showed that LDH nanoparticles are taken up by developing pollen. Using β-glucuronidase (GUS) transgene as the reporter, we found that LDH-delivered functional dsRNA efficiently induces RNAi of the GUS gene and reduces the GUS enzyme activity. Our findings have thus demonstrated that an LDH delivery platform with a size of up to 50 nm in diameter can facilitate the delivery of functional exogenous dsRNA into intact plant cells.

Results

Characteristics of LDH nanoparticles

The good dispersion and typical hexagonal morphology of prepared LDH nanoparticles were illustrated in transmission electron microscopy (TEM) images (Figure 1A). The nanoparticles showed the increasing size and narrow particle size distributions with the polydispersity index values being between 0.152 and 0.246 (Figure 1B; Supplemental Table S1). The Z-average particle size obtained with the dynamic light scattering (DLS) was 32.7 ± 2.2, 52.1 ± 3.7, 80.7 ± 3.6, and 122.9 ± 3.2 nm for the four samples, which we subsequently refer to as LDH-30, LDH-50, LDH-80, and LDH-120 (Supplemental Table S1), respectively. The Z-average particle sizes are very much consistent with the mean lateral dimensions from TEM images being around 26.6 ± 9.3, 47.3 ± 17.7, 70.6 ± 20.1, and 117.5 ± 29.4 nm for LDH-30, LDH-50, LDH-80, and LDH-120, respectively. These LDHs were all positively charged in deionized water, with the Zeta potential being 38.6 ± 2.2, 43.7 ± 1.4, 41.6 ± 1.7, and 47.9 ± 3.3 mV, respectively (Supplemental
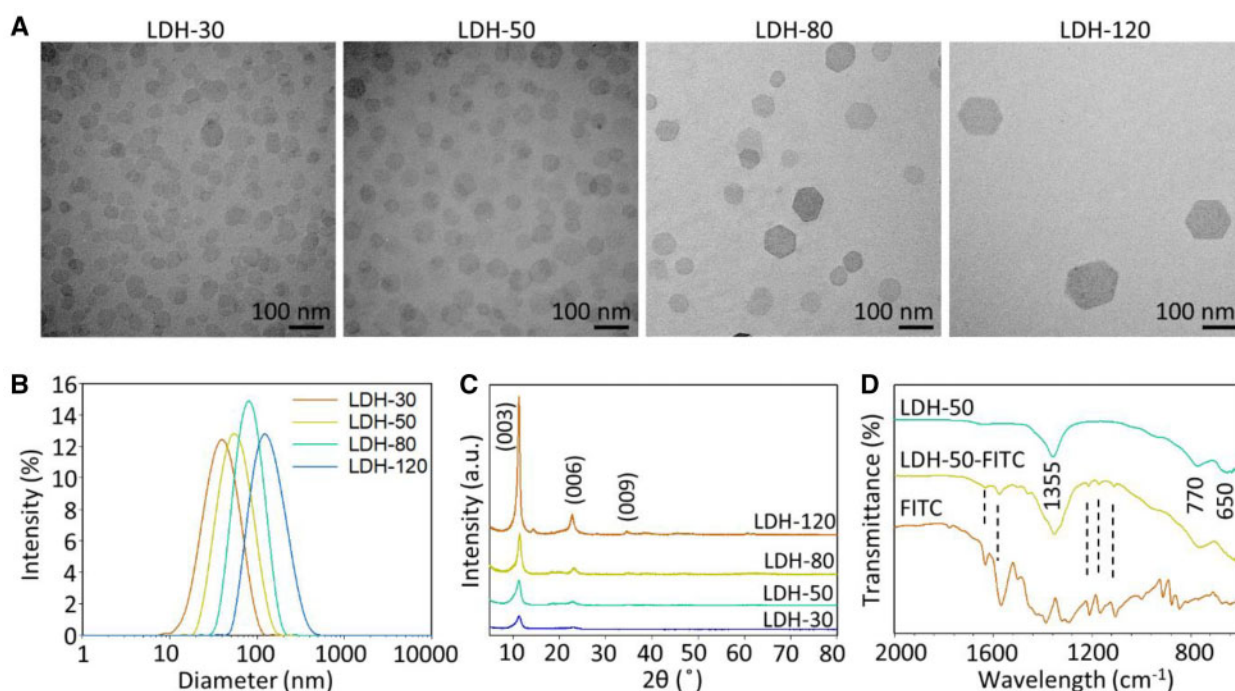
Figure 1 Characteristics of LDH nanoparticles. A, TEM images of LDHs. B, DLS particle size distributions. C, XRD patterns, numbers above the lines indicating crystal facet corresponding to diffraction peaks. D, FTIR spectra, number within the lines indicating absorption wavelength of corresponding peaks, dash lines indicating matched peaks between FITC and LDH-50-FITC.

Table S1). The positive surface charges enable nanoparticles to carry negatively charged cargoes, such as negatively charged nucleic acids.

The X-ray diffraction (XRD) pattern (Figure 1C) shows the typical characteristic reflections on planes (003), (006), and (009) for LDH materials. The peaks became intensified, and their width narrower, from LDH-30 to LDH-120, indicating the improved crystallinity of larger LDH nanoparticles. The average thickness of LDH crystals along the c axis was 6.0, 7.1, 9.9, and 15.3 nm for LDH-30, LDH-50, LDH-80, and LDH-120, respectively, as estimated from the full width at half maximum of (003) diffraction using the Scherrer Equation (Patterson, 1939). Comparison of the TEM lateral dimension and the estimated thickness along the c axis indicates the aspect ratio of these LDH nanoparticles was 5–8, in accordance with our previous report (Xu et al., 2007). The Fourier-transform infrared (FTIR) spectrum (Figure 1D) of LDH-50 alone shows a broad peak at around 1,355 cm^{-1}, which we tentatively assigned to NO_3^- as well as CO_3^{2-} located in the interlayer wherein the latter was formed from aerial CO_2 (Dong et al., 2014). Peaks at around 770 and 650 cm^{-1} are normally assigned to vibration modes of M-O and M-O-H in the metal hydroxide matrices (Xu and Zeng, 2001). In particular, fluorescein isothiocyanate (FITC)- labeled LDH-50 (LDH-50-FITC) basically shows similar FTIR peaks to that in LDHs, while some finger-printing peaks around 1,100–1,300 and 1,500–1,700 cm^{-1} were identified

and attributed to stretching vibrations of C–O, C=C, and C=O bonds in FITC, indicating the successful labeling of LDH nanoparticles with FITC (Xu et al., 2008).

LDH internalization by pollen grains

Mature tomato pollen was incubated in a solution containing FITC-labeled LDH nanoparticles of different sizes to investigate whether the LDH nanoparticles are internalized by the mature pollen. After incubating mature pollen for 2 h at room temperature with FITC-labeled LDH-30 and LDH-50 nanoparticles, the pollen was clearly observed to show green fluorescence, as detected by confocal microscopy (Figure 2A). The fluorescence inside mature pollen incubated with LDH-80 was much weaker, and negligible fluorescence was seen inside pollen grains incubated with LDH-120 (Figure 2A). The fluorescence intensity change reveals that these tomato pollen grains prefer to internalize small LDH nanoparticles.

In agreement with the confocal images, the quantitative mean fluorescence intensity (MFI) of pollen grains incubated with LDH nanoparticles at the concentration of 50 mg/L for 2 h (Figure 2B) was 11.2 ± 1.0, 9.4 ± 1.0, 5.5 ± 0.4, and 1.5 ± 0.1 times the MFI of untreated control pollen (1.0) for LDH-30, LDH-50, LDH-80, and LDH-120, respectively. The MFI changes confirm the key role of the LDH nanoparticle size, and the smaller LDH nanoparticles were internalized into the mature pollen grains much more efficiently than
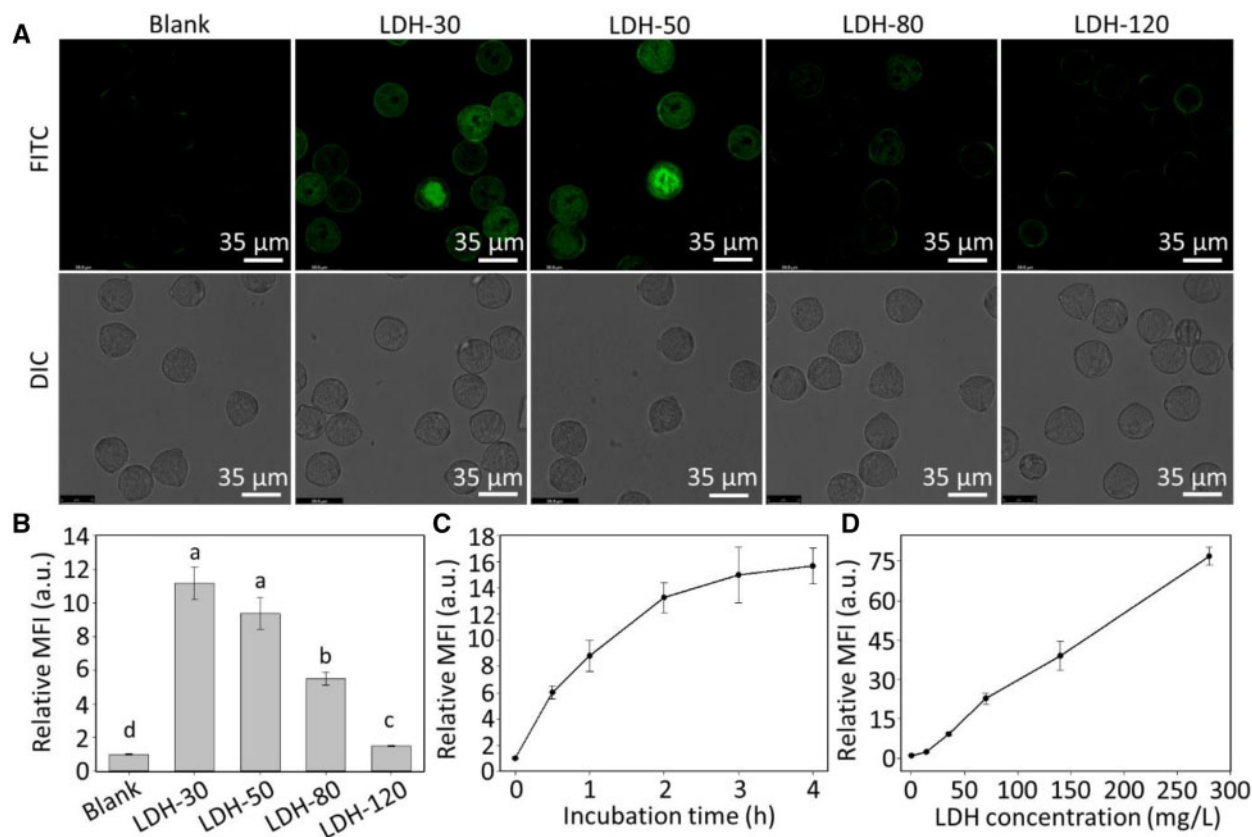
Figure 2 Internalization of LDH nanoparticles of different sizes by mature pollen. A, Confocal microscope images (FITC and DIC: differential contrast channel) of mature pollen after treatment with LDH-FITC at 50 mg/L for 2 h at room temperature. B, MFI of mature pollen collected by flow cytometry after treatment with LDH-FITC at 50 mg/L for 2 h; different lower-case letters indicate significant differences of $P < 0.05$ by t test between treatments. C, Time-dependent uptake of 50 mg/L of LDH-50 by mature pollen. D, Dose-dependent uptake of LDH-50 by mature pollen after 2 h of incubation. Pollen grains were collected from floral buds >10 mm in length. B–D, Data are shown as mean ± SEM ($n = 3$). The MFI values are expressed relative to the autofluorescence of the pollen (blank treatment).

the larger ones. Given the MFI increase is almost linear in relation to the fraction of LDH nanoparticles smaller than 50 nm in all four LDH samples (Supplemental Figure S1), the upper size limit of LDH nanoparticles taken up by mature pollen grains appears to be around 50 nm.

We also examined the time-dependent uptake of LDH-50 nanoparticles over a 4-h incubation period (Figure 2C). The MFI of pollen incubated with 50 mg/L of LDH-50 nanoparticles increased rapidly over the first 30 min of incubation but continued to increase substantially until 2 h of incubation. Interestingly, the time-dependent internalization profiles for LDH-30 and LDH-50 were not significantly different (Supplemental Figure S2). Similarly to that reported for mammalian cells (Oh et al., 2009), the fluorescence with LDH-30 nanoparticles decays more quickly than that with LDH-50 nanoparticles in pollen (Supplemental Figure S3), and hence LDH-50 nanoparticles were chosen for most subsequent experiments. The uptake of LDH-50 nanoparticles by mature pollen was also dose-dependent (Figure 2D). The MFI increase was almost linear in relation to the nanoparticle concentration up to nearly 300 mg/L.

The biocompatibility of LDH nanoparticles was further investigated in terms of the in vitro germination rate in the presence of LDH nanoparticles as an indicator of pollen viability (Shivanna and Heslopharrison, 1981). As shown in Supplemental Figure S4, the germination rate was around 97% in the standard conditions, which slightly decreased to around 90% in the presence of 50–500 mg/L of LDH-50 nanoparticles. These data illustrate that LDH nanoparticles have minimum side effects on the pollen germination process, indicating high biocompatibility of LDH nanoparticles with plant cells, as has been reported for animal cells (Xu et al., 2008; Gu et al., 2018).

Effect of low temperature and endocytosis inhibitor on uptake of LDH nanoparticles

Understanding the pollen uptake mechanism of nanoparticles is important for designing nanoparticle platforms for delivery to plants. To this end, cold treatment at 4°C and endocytosis inhibitors were applied during the uptake of LDH-50 nanoparticles by mature pollen. As shown in Figure 3A, the MFI of pollen grains treated at 4°C was reduced to <50% of MFI of pollen incubated at room temperature,
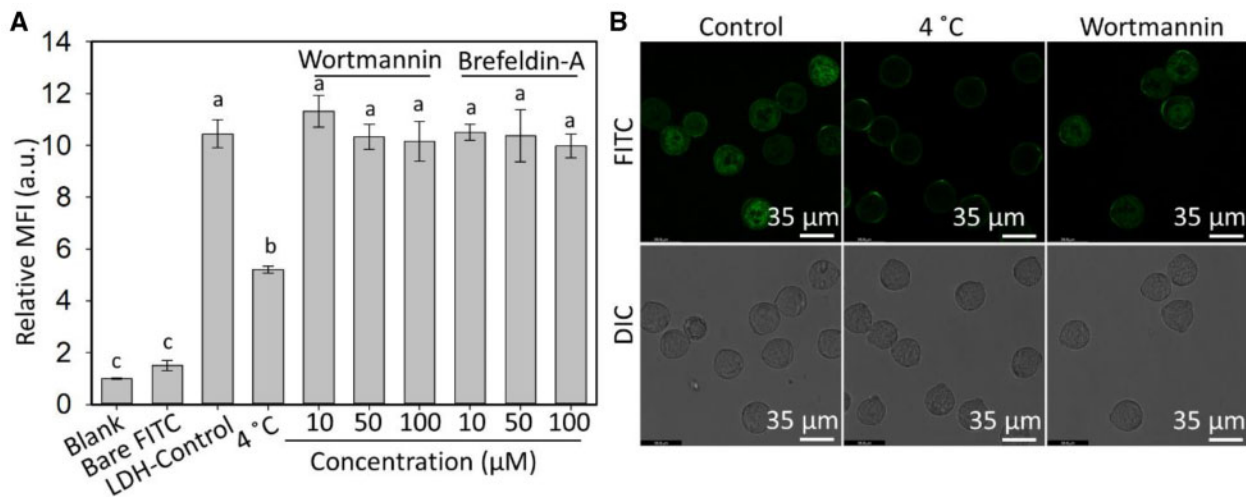
Figure 3 Pathways of LDH internalization by mature pollen grains. A, Insignificant effect of Wortmannin and Brefeldin-A (10–100 µM) on the uptake of LDH-50-FITC (50 mg/L) by mature pollen after 2 h of incubation at room temperature. In contrast, uptake of LDH-50-FITC by mature pollen after 2 h of incubation at 4°C was significantly lower than at room temperature (LDH-Control). Data are based on flow cytometry measurements (mean ± sem of three biological replicates) and the MFI values are expressed relative to the autofluorescence of untreated pollen (Blank treatment). Uptake of an equivalent amount of free FITC not in complex with LDH-50 (Bare FITC) was not significantly different from the Blank control. The lower-case letters indicate significant differences of $P < 0.05$ between groups by t test. B, Confocal microscope images of mature pollen after treatments with LDH-50-FITC at room temperature (Control), LDH-50-FITC at 4°C and LDH-50-FITC plus Wortmannin (100 µM) at room temperature. Mature pollen grains were collected from fully opened flowers (floral buds >10 mm in length).

which was also reflected by the much weaker green signals in the FITC channel in confocal microscope images (Figure 3B; Supplemental Figure S5), which indicate the pollen uptake of LDH nanoparticles is inhibited by cold treatment. Less uptake at 4°C suggests that nanoparticle uptake by pollen grains is partly energy-dependent. To further investigate what type of energy-dependent endocytosis is involved, two plant endocytosis regulators were used in the pollen uptake test (Aniento and Robinson, 2005; Wang et al., 2005; Reynolds et al., 2018). Wortmannin interacts with the receptor on the cell membrane to inhibit clathrin-mediated endocytosis, whereas Brefeldin-A interrupts the recycling of proteins to the plasma membrane during exocytosis. Brefeldin-A is also reported to enhance *Picea meyeri* pollen tube endocytosis (Wang et al., 2005). As shown in Figure 3A and B, and Supplemental Figure S5, co-incubation with either inhibitor did not affect the pollen uptake of LDH-50, indicating neither clathrin-mediated endocytosis nor exocytosis contributes to the LDH internalization by pollen grains.

Uptake of LDH nanoparticles by pollen at different stages of development

Pollen at five stages of development was collected from tomato floral buds and flowers (Polowick and Sawhney, 1993), namely, monocellular pollen extracted from flower buds 4–6 mm in length when the developing petals and sepals are tightly closed; early bicellular pollen from flower buds 6–8 mm in length when the sepals were slightly separated but the petals were still closed; bicellular pollen from flower

buds 8–10 mm in length when the flowers were just starting to open; late bicellular pollen extracted from fully open flowers with anthers >10 mm in length; and mature pollen collected from dehiscing anthers (Figure 4A). The DNA staining dye Hoechst 33342 was applied for visualization of the nuclei within the pollen (Figure 4B; Supplemental Figure S6B).

Early bicellular pollens (from 6 to 8 mm flower buds) internalized the largest amount of LDH-50 nanoparticles, as determined by both MFI measurements from flow cytometry data and confocal microscope images (Figure 4C and D). Relatively to the level of auto-fluorescence, the MFI of pollen of all stages was increased by at least four times after 2-h incubation with LDH-50 nanoparticles. Specifically, early bicellular pollen collected from 6 to 8 mm flower buds showed the highest MFI (19.4 ± 1.8), more than twice that of monocellular pollen collected from 4 to 6 mm flower buds (8.2 ± 0.6; Figure 4C). From the maximum observed for early bicellular pollen, the MFI gradually declined as the pollen matured, and the lowest MFI was for mature dehisced pollen (4.2 ± 1.1; Figure 4C). These MFI results were confirmed by the FITC green fluorescence observed in the confocal images of the developing pollen (Figure 4D). The internalization of LDH-50 nanoparticles was further investigated using confocal z-stacking imaging, which confirmed that the green fluorescence was emitted from the inside and not the surface of the pollen (Supplemental Figure S7). In summary, our data clearly demonstrate that early bicellular pollen internalize more LDH-50 nanoparticles than monocellular, late bicellular,
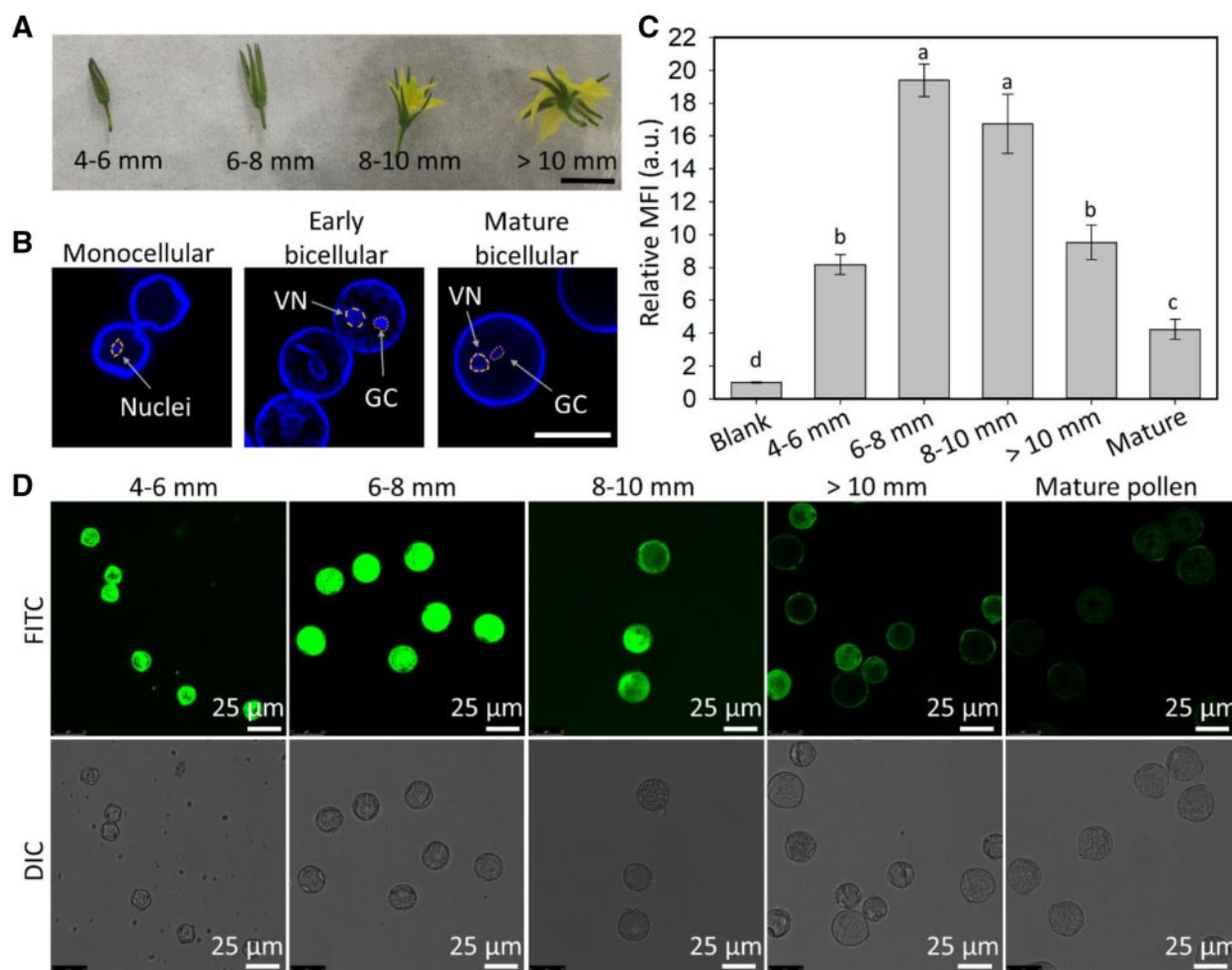
Figure 4 Internalization of LDH-50 nanoparticles by pollen at different stages of development. A, Representative images of flowers collected at four stages (scale bar, 10 mm). B, Confocal microscope images of monocellular, early and mature bicellular pollen nuclei stained with Hoechst 33342 (VN: vegetative nuclei, GC: generative cell, circles indicate the area of VN and GC, scale bar, 25 μm). C, Flow cytometry data, where lower-case letters indicate a significant difference of $P < 0.05$ between treatments. Data are shown as mean $\pm$ SEM for $n = 3$ biological replicates. D, Confocal microscope images of pollen at different stages of development after incubation for 2 h at room temperature with 50 mg/L of LDH-50-FITC.

and mature pollen, and therefore, early bicellular pollen was used in our subsequent experiments.

LDH nanoparticles enhance the delivery of dsRNA into pollen

To test the capability of LDH nanoparticles to facilitate the uptake of dsRNA, Cucumber Mosaic Virus dsRNA was synthesized and labeled in vitro with Cy3 (dsRNA-Cy3, 300 bp, sequence provided in Supplemental Dataset S1; Mitter et al., 2017) and loaded onto LDH-50 at a mass ratio of LDH:dsRNA = 10:1 (LDH–dsRNA). When early bicellular pollen was incubated for 2 or 12 h with dsRNA-Cy3 alone, negligible fluorescence increases were observed in the pollen (Figure 5A and B). In contrast, pollen incubated with LDH–dsRNA at the same concentration of dsRNA-Cy3 for 2 and 12 h showed significant increases in the MFI, i.e. by ∼31% and ∼37%, respectively (Figure 5A and B). The percentage of Cy3-positive pollen after 2- and 12-h incubation with

dsRNA-Cy3 was only 0.79% $\pm$ 0.34% and 0.94% $\pm$ 0.07%, respectively, which significantly increased to 2.85% $\pm$ 0.13% and 6.39% $\pm$ 0.92% for pollen incubated with LDH–dsRNA for the same incubation periods, respectively (Figure 5C and D). Nevertheless, our data clearly show that LDH-50 nanoparticles enhance the pollen internalization of dsRNA and indicate that LDH nanoparticles appear an effective platform for nucleic acid delivery into plant cells.

LDH nanoparticles facilitate dsRNA uptake and induction of RNAi in pollen

We next tested whether LDH nanoparticles can deliver functional dsRNA to induce gene silencing in early bicellular pollen. For this purpose, a GUS transgene encoding β-glucuronidase in the transgenic tomato line 10512i was selected as the target gene (Carroll et al., 1995; Keddie et al., 1998), and a 505-bp GUS dsRNA was synthesized in vitro (Mitter et al., 2017; sequence provided in Supplemental
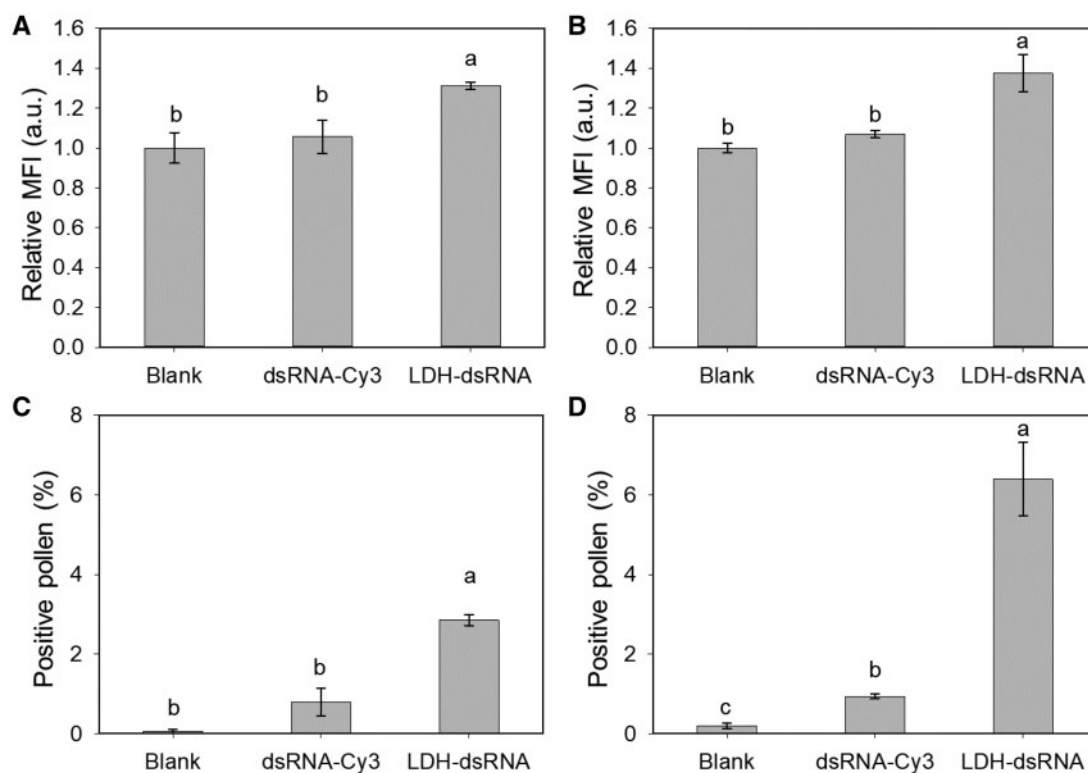
Figure 5 LDH-50 facilitated uptake of dsRNA by early bicellular pollen. MFI of pollen treated with Cy3-labeled 300-bp RNA (dsRNA-Cy3) and LDH-50 conjugated with dsRNA-Cy3 (LDH–dsRNA) after incubation for 2 h (A) and 12 h (B). The concentrations of LDH-50 and dsRNA used were 100 and 10 mg/L, respectively. The MFI values are expressed in relation to the autofluorescence of the pollen (Blank treatment). The percentage of positive pollen (above gate 42,000 on the flow cytometer setting) after incubation with dsRNA-Cy3 and LDH–dsRNA for 2 h (C) and 12 h (D) at room temperature. A–D, Different lower-case letters indicate a significant difference of $P < 0.05$ between treatments by t test. Data are shown as mean $\pm$ SEM for $n = 3$ biological replicates. Early bicellular pollen grains were collected from 6 to 8 mm flower buds.

Dataset S2). As shown in Supplemental Figure S8, most dsRNA was loaded onto LDH-50 nanoparticles (LDH–dsRNA) at the LDH:dsRNA mass ratio of 3:1 to 5:1.

After incubation with blank LDH-50 (denoted as LDH), GUS dsRNA alone, or LDH-50–dsRNA (denoted as LDH–dsRNA), the early bicellular pollen was subjected to a modified fluorometric 4-methylumbelliferyl β-D-glucuronide (MUG) assay and assessed by flow cytometry for quantification. β-glucuronidase converts MUG into the fluorescent product 4-methylumbelliferone (MU) as the indicator of GUS activity. The quantitative MU MFI data (Figure 6A) show that the pollen incubated with LDH–dsRNA (20 mg/L of dsRNA and the LDH:dsRNA mass ratio of 3:1) for 3 d decreased the level of MU fluorescence intensity to 83.6% $\pm$ 3.0% of the untreated GUS positive control pollen. This is likely to be an underestimate of the effect of LDH:dsRNA on the GUS activity because the pollen extracted from a GUS-negative, nontransgenic tomato line showed autofluorescence and an MUI of 36.6 $\pm$ 3.1% of untreated GUS-positive control pollen (Figure 6A). We observed no significant change in the MU fluorescence intensity for early bicellular pollen incubated for 3 d with LDH-50, GUS dsRNA alone, and green fluorescence protein (GFP) dsRNA compared with untreated GUS-positive control pollen. These data clearly demonstrate that the LDH–dsRNA complex

specifically downregulates β-glucuronidase activity encoded by the GUS transgene in pollen.

As shown in Figure 6B, the early bicellular pollen treated with GUS dsRNA loaded to LDH-30 and LDH-50 exhibited a significant decrease in the MU fluorescence intensity after 3 d of treatment to 89.1% $\pm$ 1.8% and 83.6% $\pm$ 3.0%, respectively, of the untreated GUS-positive control pollen. In comparison, treatment with LDH-80–dsRNA showed an insignificant decrease in MFI to 90.8 $\pm$ 4.2% of untreated GUS-positive control pollen. Thus, LDH-50 nanoparticles are the most suitable vehicle for dsRNA delivery into early bicellular tomato pollen to silence the target gene, which is consistent with the upper size limit of around 50 nm for LDH nanoparticles for pollen uptake, and rapid biodegradation of 30-nm LDH nanoparticles in pollen.

The effects of the LDH-50:dsRNA mass ratio and the dsRNA concentration were further investigated. Figure 6C shows that early bicellular pollen incubated with LDH–dsRNA at 2:1 reduced the MFI to 93.9% $\pm$ 2.5%, while the MFI was significantly reduced to 86.0% $\pm$ 2.6%, 84.0% $\pm$ 3.0%, and 84.1% $\pm$ 3.5% for pollen incubated with LDH–dsRNA at 3:1, 4:1, and 5:1, respectively. There was no significant difference between pollen treated with LDH–dsRNA at mass ratios of 3:1, 4:1, and 5:1. As mentioned earlier and shown in Supplemental Figure S8, dsRNA was
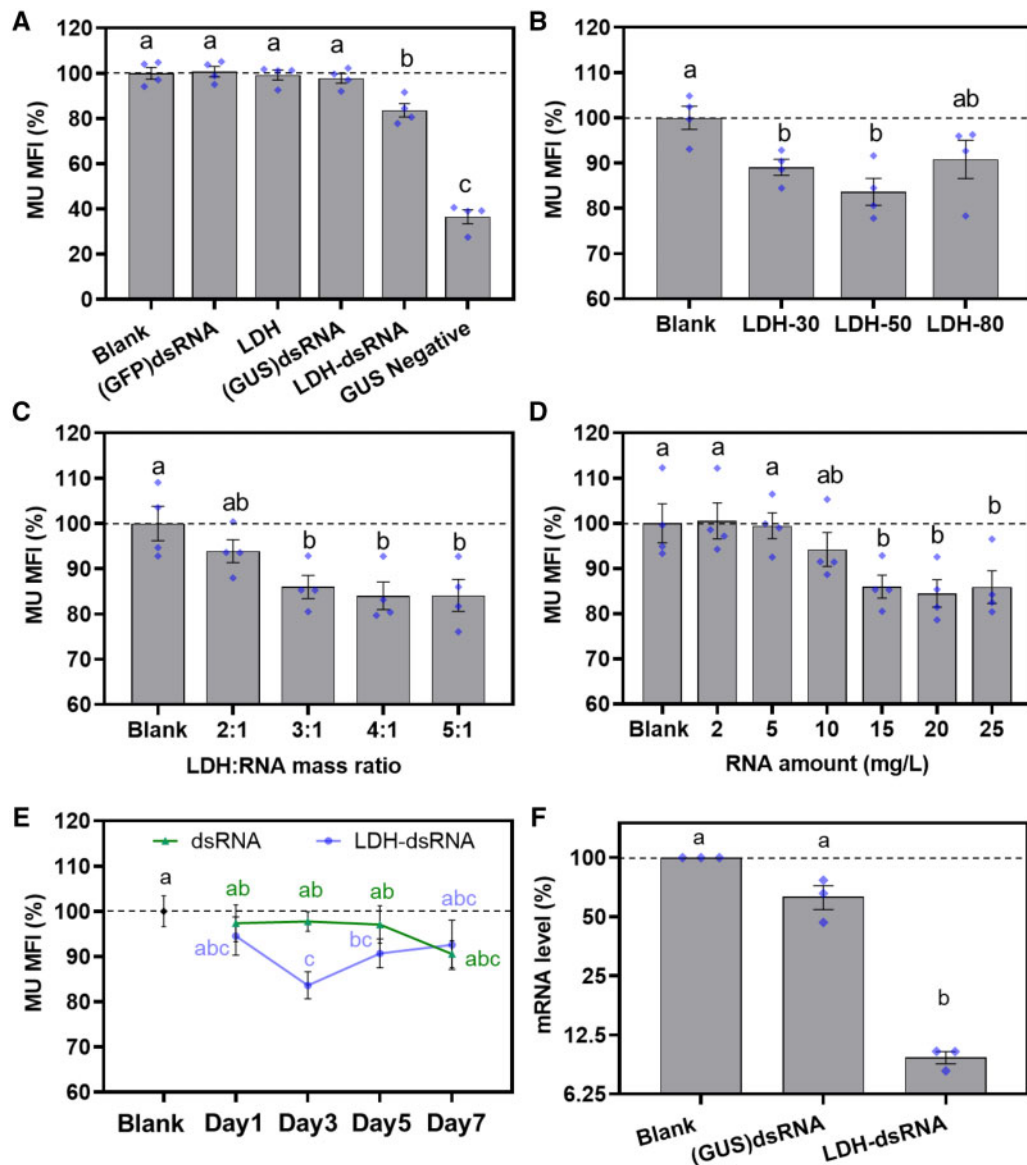
Figure 6 LDH-50–dsRNA induced silencing of the *GUS* reporter gene in early bicellular pollen. A, Decreased levels of GUS protein after 3-d incubation at 20 mg/L of dsRNA loaded on 60 mg/L of LDH-50; GUS protein levels were measured by a fluorometric MUG assay. The non-treatment group denoted as Blank, non-specific GFP dsRNA-treated group denoted as (GFP)dsRNA, LDH alone treated group denoted as LDH, Bare *GUS* dsRNA-treated group denoted as (GUS)dsRNA, LDHs conjugated *GUS* dsRNA treated group denoted as LDH–dsRNA, results from no-treated wild-type (non-*GUS* transgenic) group denoted as GUS negative. B, Effect of the LDH particle size on suppression of GUS protein levels after 3-d incubation at 20 mg/L of dsRNA (60 mg/L of LDH). C, Effect of the LDH:RNA mass ratio on suppression of GUS protein levels after 3-dy incubation at 15 mg/L of dsRNA. D, Effect of the dsRNA dose on suppression of GUS protein levels after 3-d incubation with the LDH:RNA mass ratio of 3:1. E, Effect of incubation period on suppression of GUS protein levels after incubation of pollen with 20 mg/L of dsRNA or with 20 mg/L of dsRNA loaded on 60 mg/L of LDH-50 (LDH–dsRNA). Data are shown as mean ± SEM for $n = 4$ biological replicates. F, RT-qPCR analysis of *GUS* mRNA levels in pollen incubated with 20 mg/L of dsRNA ((GUS)dsRNA) and 20 mg/L of dsRNA in complex with 60 mg/L of LDH-50 (LDH–dsRNA) for 3 d A–E, data are shown as mean ± SEM for $n = 4$ biological replicates (blue diamonds) and F, data are shown as mean ± SEM for $n = 3$ biological replicates (blue diamonds). Pollen grains were collected from 6 to 8 mm flower buds. Different lower-case letters indicate a significant difference with $P < 0.05$ between groups by t test.

fully loaded onto LDH-50 at the mass ratio of 3:1, 4:1, and 5:1, while there was some unloaded dsRNA at the mass ratio of 2:1 that migrated to the gel bottom under the electric field. The unloaded dsRNA in the case of the mass ratio 2:1 was most likely not taken up by the pollen, resulting in an insignificant decrease in β-glucuronidase

activity compared with the untreated *GUS*-positive control pollen.

The data for the dsRNA dose effect are shown in Figure 6D. At the dsRNA dose of 2–5 mg/L, the GUS activity was not affected in the early bicellular pollen after 3 d of incubation with LDH–dsRNA. Clearly, 10 mg/L of dsRNA in the

LDH–dsRNA form decreased the MU fluorescence intensity to 94.2% ± 3.7% of the untreated *GUS*-positive control pollen after 3 d of incubation, but the decrease was not significant. The MFI decreased to 86.0% ± 2.6%, 84.4% ± 3.0%, and 85.8% ± 3.6% of the untreated *GUS*-positive control pollen when the dsRNA dose was increased to 15, 20 and 25 mg/L, respectively. Therefore, it seems that the optimal dsRNA concentration for inhibition of GUS activity was 15–20 mg/L. However, increasing the dsRNA dose from 20 to 25 mg/L did not further enhance the inhibition of GUS activity, which is a similar saturation phenomenon to that reported for other examples of RNAi induced by topical application of dsRNA (McLoughlin et al., 2018).

The LDH–dsRNA-induced GUS activity inhibition is a time-dependent process. As shown in Figure 6E, the MU fluorescence intensity of early bicellular pollen did not change significantly during a 7-d incubation with 20 mg/L of dsRNA alone. In sharp contrast, the MFI of pollen treated with 20 mg/L of dsRNA in complex with LDH-50 decreased significantly and reached 83.6% ± 3.0% of the untreated *GUS*-positive control pollen after 3 d of treatment. Subsequently, the MU fluorescence intensity recovered slightly to 90.2% ± 4.0% and 92.5% ± 5.5% at days 5 and 7, respectively. By day 7, both the dsRNA- and LDH–dsRNA-treated groups were not significantly different from the untreated *GUS*-positive control pollen (Figure 6E).

Assessing the effect of LDH–dsRNA on inhibition of GUS activity is an indirect indicator of silencing of the *GUS* transgene, and is dependent on the stability of the GUS protein, which may underestimate the level of RNAi. To address this issue, quantitative reverse transcription polymerase chain reaction (RT-qPCR) was used to quantify *GUS* mRNA levels in early bicellular pollen incubated with naked *GUS* dsRNA and *GUS* dsRNA in complex with LDH-50. Incubation of pollen with 20 mg/L of naked *GUS* dsRNA for 3 d resulted in a 36.7% ± 8.8% decrease in *GUS* mRNA levels compared with the untreated *GUS*-positive control pollen (Figure 6F). In sharp contrast, treatment with 20 mg/L of *GUS* dsRNA in complex with LDH-50 for 3 d caused a highly significant decrease (89.2 ± 1.9%) in *GUS* mRNA levels. Our results clearly demonstrate that LDH-50 nanoparticles facilitate the delivery of dsRNA into developing pollen to efficiently induce RNAi.

Discussion

Nanoparticles have been extensively studied for diagnostic, therapeutic, and drug delivery purposes in mammalian systems. However, very few studies have demonstrated the application for the delivery of biomolecules into intact plant cells. Furthermore, developing a better understanding of nanoparticle–plant interactions is required to enable the design of nanoparticle delivery platforms for the modification of plant physiology. In this research, we have demonstrated that LDH nanoparticles with an average particle diameter of 50 nm or smaller are readily taken up by pollen, and moreover, significantly facilitate the uptake of dsRNA by developing pollen to efficiently induce RNAi. We have also confirmed that LDH-50 nanoparticles were internalized by 1-week-old Arabidopsis roots (Supplemental Figure S9), suggesting that small LDH nanoparticles could be used in the future to facilitate the delivery of biomolecules into whole plants and tissues.

LDH nanoparticles with the average diameters of 30 and 50 nm showed the most rapid internalization, indicating that the particle size is one of the key factors that affect the nanoparticle internalization by plant cells (Lv et al., 2019). Our further analyses showed that the pollen uptake is well correlated with the portion of <50 nm LDH nanoparticles at the same dose (Supplemental Figure S1), suggesting that the upper size limit for tomato pollen internalization is around 50 nm. The plant cell membrane is reported to allow the uptake of nanoparticles of <500 nm in size (Wang et al., 2016; Demirer et al., 2019). Due to the dynamic nature of pectin in the cell wall, nanoparticles of around 50 nm or smaller are reported to traverse the cell wall, enter the cytoplasm of intact plant cells and translocate within plants (Dan et al., 2015; Wang et al., 2016; Demirer et al., 2019; Avellan et al., 2019; Sun et al., 2020). Nanoparticle surface chemistry also affects the interactions of nanoparticles with the cell wall and the subsequent endocytosis by plant cells (Avellan et al., 2019; Hu et al., 2020). To our knowledge, no size exclusion limit has been reported for the uptake of nanoparticles by developing pollen yet probably due to the complexity of the pollen wall. Based on this research, we believe that the dynamic size exclusion limit of tomato pollen is around 50 nm, which is similar to that for some other plant cells (Dan et al., 2015; Schwab et al., 2016; Sun et al., 2020).

In addition to overcoming the obstacle of the plant cell wall, the uptake mechanism into the cell is another factor key to developing nanoparticle delivery platforms for plants. Both energy-dependent and energy-independent LDH uptake processes appeared to be operating in pollen. As reported previously, delaminated LDH nanosheets of 30 nm in diameter and 0.5–2 nm in thickness diffused into tobacco (*N. tabacum*) cv Bright Yellow 2 cells (Bao et al., 2016). As the hydrodynamic size of our LDH-30 and LDH-50 nanoparticles is very similar to that of reported LDH nanosheets, it is reasonable to infer that LDH-30 and LDH-50 nanoparticles penetrate pollen by a process of diffusion. Interestingly, carbon nanotubes were proposed to directly penetrate the plant cell membrane and chloroplast via a lipid exchange envelope penetration process (Giraldo et al., 2014; Wong et al., 2016), which may work for other nanoparticles with a strong surface charge (Lew et al., 2018), including LDH nanoparticles. This kind of direct penetration bypassing the endocytosis and endosomal vesicle may contribute to the energy-independent uptake of LDH nanoparticles by tomato pollen. While clathrin-mediated endocytosis seems not to be responsible for LDH uptake by pollen grains (Figure 3), more investigations into the nanoparticle uptake mechanism by the intact plant cells are needed in the future.

Interestingly, pollen at different stages of development shows different uptake behaviors. We found that the early bicellular pollen takes up the most amount of LDH-50 nanoparticles while mature pollen grains internalize much less. The different uptake rates may be attributed to the changing wall structure of developing pollen. Mature pollen grains are protected by a bilayered wall composed of the inner intine layer and the outer exine layer (Polowick and Sawhney, 1993a, 1993b; Figure 7). The intine is made largely of cellulose and is structurally very similar to most other plant cell walls, whereas the exine is composed mostly of sporopollenin, which is one of the most stable and chemically inert hydrocarbon polymers in nature. Furthermore, there are differences in the timing of deposition of the intine and exine during pollen development. The outer exine starts to be laid down early in the monocellular stage and continues to thicken during tomato pollen development (Polowick and Sawhney, 1993a, 1993b). In contrast, the internal intine only starts to form at the early bicellular stage of tomato pollen development (Polowick and Sawhney, 1993a, 1993b). These changes in the wall structure during pollen development, including maturation of the inner intine layer and/or the thickened exine layer, may affect nanoparticle permeability and explain why pollen at different stages of development show different capacities to take up LDH nanoparticles.

In conclusion, we have also demonstrated that LDH-50 nanoparticles can deliver a biologically active molecule into developing pollen. LDH-50 nanoparticles efficiently enhanced the uptake of dsRNA by the developing pollen. Furthermore, LDH-50 nanoparticles delivered *GUS* dsRNA to efficiently silence the *GUS* reporter gene in the developing pollen. Treatment for 3 d with LDH–dsRNA caused a 16.7% decrease in GUS protein activity while no significant changes

were identified with dsRNA alone after 7 d of treatment. A slight decrease in GUS activity levels was observed at day 7 in the naked dsRNA treated group, which may be caused by a few reasons. The slow yet accumulative uptake of naked dsRNA may start to reduce the GUS protein activity after day 7. However, the impact of gene silencing is also affected by the relatively high stability of GUS protein. Indeed, the naked dsRNA treatment lowered *GUS* mRNA levels by ~37% at day 3 (Figure 6F), whereas the impact on GUS protein activity was barely detectable, if at all, after 7 d of treatment (Figure 6E).

Most notably, treatment of early bicellular pollen for 3 d with LDH–dsRNA caused an 89% decrease in *GUS* mRNA levels (Figure 6F). dsRNA internalization facilitated by LDH-50 nanoparticles can probably be attributed to three reasons (Figure 7). First, loading dsRNA onto LDH nanoparticles masks the negative charge of dsRNA so that LDH–dsRNA complexes penetrate through the negatively charged phospholipid cell membranes and exine much more easily than free negatively charged dsRNA (Bohne et al., 2003). Secondly, dsRNA loaded onto LDHs increased the stiffness of the dsRNA compared with free dsRNA, which may help the internalization process by facilitating the movement of dsRNA molecules through pores in the pollen wall and the plant cell membrane (Zhang et al., 2019). Thirdly, during the uptake process, LDH nanoparticles can protect fragile dsRNA from nucleases and degradation, as seen in this research (Supplemental Figure S8B) and the previous report (Mitter et al., 2017; Demirer et al., 2020). In short, LDH-mediated delivery is a quick and efficient process for potentially modifying traits in plant cells.

Our findings suggest that the bio-compatible smaller LDH nanoparticles can serve as a simple biomolecule delivery
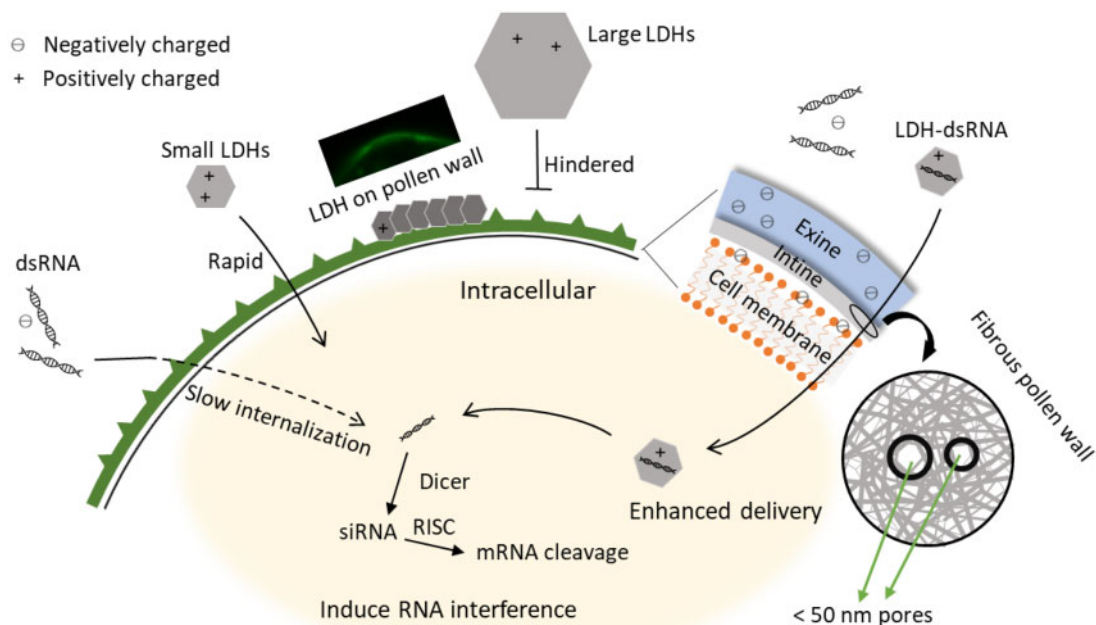
Figure 7 Schematic illustration of LDH nanoparticles facilitating pollen uptake of dsRNA. RISC, RNA-induced silencing complex.

tool for fundamental plant science research in model plant cell systems, and are a potential vector for non-GM trait manipulation in plants, including protection against viruses based on RNAi technology (Mitter et al., 2017) and engineering metabolic pathways in plants.

Methods

Synthesis of LDH nanoparticles

MgAl LDHs with an average particle size from 50 to 120 nm were prepared via co-precipitation followed by hydrothermal treatment at 100°C for different time periods (Xu et al., 2006). Briefly, for LDHs with an average size of 50 nm, co-precipitation was carried out by adding mixed $Mg(NO_3)_2$ and $Al(NO_3)_3$ solution into NaOH solution under vigorous stirring for 10 min, then the LDH precipitates were collected via centrifugation, washed twice and homogeneously dispersed in deionized water after standing 7 d with occasional shaking. These LDH nanoparticles were then heated in an autoclave at 100°C to grow larger, with the average particle size increasing from 50 to 80 or 120 nm after 8 or 72 h, respectively; particles were denoted as LDH-50, LDH-80, and LDH-120. LDHs with an average size of 30 nm were prepared similarly for LDH-50, except the co-precipitation process was conducted in methanol solution. The prepared LDH nanoparticles were resuspended in deionized water after washing. Solid samples of all prepared LDHs were obtained with lyophilization for characterization.

FITC-labeled LDHs were prepared by adding LDH nanoparticle suspension of different sizes drop wise into FITC solution (NaOH water solution, pH ∼11) at a mass ratio of 20:1 (LDH: FITC), and the mixture was stirred for 1 h at room temperature, followed by centrifuging and washing thrice to remove excessive FITC, and then particles were monodispersed in deionized water similarly.

Characterization of LDH nanoparticles

All LDH suspensions were subjected to a Nano Zetasizer for size distribution and surface charge measurement by the dynamic light scattering method. TEM images of LDHs of different sizes were collected on JEOL JSM-2010 TEM at the operating voltage of 100 kV. FTIR spectra of solid nanoparticle samples were recorded in a Nicolet 6700 FTIR device by scanning 32 times in the range of 500–4,000 cm^{-1} at the resolution of 2 cm^{-1}. XRD patterns of solid samples were obtained in a Rigaku Miniflex X-ray diffractometer at a scanning rate of 2°/min with 2θ ranging from 10° to 80° using Cu Kα radiation. The thickness of these LDH crystallites was estimated based on the Scherrer equation, $D = (k \times \lambda)/(\beta/360 \times \cos\theta)$, where D is the average thickness, k the constant (0.89), λ the radiation wavelength (0.154 nm), β the full width at half maximum, and θ the Bragg angle of (003) or (006) diffraction. The average lateral dimension was calculated based on the lateral measurement of 50–100 nanoparticles for each sample in TEM images.

Plant growth and pollen collection

Tomato seeds (variety Money maker nontransgenic wild-type and the transgenic line *sAc 10512i GUS* homozygotes (Carroll et al., 1995; Keddie et al., 1998)) were germinated in water, the seedlings were grown in nursery trays in a glasshouse at the day temperature of 24–26°C and the night temperature of around 20°C (16 h/8 h with artificial lights) for 3–4 weeks, and then transferred to large pots with the potting mix. Pollen at different stages of development from flower buds (4–6 mm, 6–8 mm, and 8–10 mm) and mature pollen from fully opened flowers (>10 mm) were collected in 10% (v/v) glycerol aqueous solution by gently breaking the detached anther with surgical blades. Mature pollen grains were also collected with a pollinator by just vibrating anthers of mature (fully opened) flowers.

Pollen nuclei staining

For pollen nuclei staining, the collected pollen was stained with 1 mg/L of Hoechst 33342 in 20 mM 2-(N-morpholino)ethanesulfonic (MES) acid buffer (pH 6.0) for 30 min in the dark at room temperature before imaging.

Pollen uptake of LDH nanoparticles

The collected pollen was transferred to 20 mM MES buffer (pH = 6.0) with LDH-FITC nanoparticles supplemented at a certain concentration. After incubation at room temperature (24°C) in the dark for 0.5–4 h, pollen was collected via centrifugation (700 rpm, 30 s), washed with fresh MES buffer three times, and then subjected to imaging in confocal microscopy (Leica SP8 confocal laser scanning microscope). For quantifying the signal from inside the pollen (average pixel intensity signal, excluding outer 0.7–1 μm of pollen in confocal image), three replicates with 10–20 pollens were measured for each treatment group. The pollens were also directly measured for fluorescence via a flow cytometer (CytoFLEX) for quantification of the fluorescence intensity.

For inhibition of uptake, the collected mature pollen grains, MES buffer and LDH-50 nanoparticle suspension were first placed at 4°C in a cold room for 1 h before uptake experiment. The uptake by mature pollen was then carried out similarly at 4°C in a cold room. For endocytosis inhibition, mature pollen grains were incubated with 10–100 μM of Wortmannin or Brefeldin-A (both stock solutions in DMSO) in MES buffer for 30 min, and then LDH-50 nanoparticles were added into the buffer for pollen grains to take up at the room temperature.

Nucleic acid loading assay and RNase protection assay

Loading of dsRNA onto LDHs was performed by carefully adding LDH nanoparticle suspensions to nucleic acid solutions, followed by pipetting up and down several times to mix. Mixed solutions with the different LDH/nucleic acid mass ratios (10:1 to 2:1) were then aged at room temperature for 2 h to allow full conjugation of nucleic acids to LDH nanoparticles via electrostatic forces. Electrophoresis mobility of nucleic acids was determined to confirm

whether nucleic acids were conjugated with LDH nanoparticles. Different mass ratios of LDHs to nucleic acids were pre-mixed at room temperature for 2 h before adding onto the loading well of the gel.

dsRNA (250 ng) conjugated with 1,250 ng of LDH (LDH–dsRNA) or without (bare dsRNA) was treated with 5 ng of RNase A (Thermal Fisher) at 37°C for 5 min. After treatment, dsRNA from LDH–dsRNA was detached with release buffer (4.11 mL of 0.2 M Na_2HPO_4 + 15.89 mL of 0.1 M citric acid; pH 3; Mitter et al., 2017) for 10 min and then added to the loading well for electrophoresis.

LDH delivery of dsRNA-Cy3 into pollen

Cucumber Mosaic Virus 2b dsRNA (300 bp) was synthesized and labeled in vitro with Cy3 (dsRNA-Cy3; Mitter et al., 2017). Collected pollen was transferred to 20 mM MES buffer (pH = 6.0) supplemented with LDH–dsRNA or dsRNA-Cy3 alone, at the dsRNA concentration of 10 mg/L and the LDH:dsRNA mass ratio at 10:1, and then incubated at room temperature in the dark for 2–12 h. Pollen was collected via centrifugation (700 rpm, 30 s), washed with fresh MES buffer three times and subjected to cytometry analysis.

LDH delivery of dsRNA to induce RNAi in pollen

LDH–dsRNA complexes were prepared by adding LDH-50 nanoparticle suspension into dsRNA solution at the LDH:dsRNA mass ratio between 2:1 and 5:1, in a way similar to that described previously. LDH-50–dsRNA, bare dsRNA and LDH-50 were added into MES buffer and incubated with collected early bicellular pollen (10512i GUS-positive) at a designed dsRNA concentration. The GUS-negative group was collected from wild-type Money Maker at the same time, and dispersed in MES buffer without adding any LDH–dsRNA, LDH-50, or dsRNA. The mixed samples were covered with aluminium foil and incubated at room temperature for 1, 3, 5, and 7 d. After incubation, the pollen was collected via centrifugation (700 rpm, 30 s), washed with fresh MES buffer three times, and subjected to staining.

Modified 4-methylumbelliferyl-β-d-glucuronide staining on pollen

The modified 4-MUG staining was conducted in MUG buffer (0.1 M pH 7.4 phosphate buffer, 10 mM ethylenediaminetetraacetic acid, 0.1% (v/v) Triton X-100, 1 mM 4-MUG). In brief, 200-μL MUG staining buffer was added to the collected treated pollen samples. The samples were covered with aluminium foil and incubated at 37°C for 24 h. The early bicellular pollen was then collected with centrifugation (700 rpm, 30 s) and washed with fresh 0.1 M pH 7.4 phosphate buffer three times for immediate flow cytometry analysis.

RT-qPCR analysis of the mRNA level

Total mRNA was extracted with the modified phenol-chloroform method, followed by reverse transcription with ProtoScript II First Strand cDNA Synthesis Kit (New England Biolabs). GUS and LAT52 (as reference) were the target genes. The qPCR was run for 40 cycles with an annealing temperature of 60°C. Data were analyzed through the ΔΔCt method to normalize the GUS mRNA level according to the LAT52 housekeeping gene and control. Primers are listed in Supplemental Dataset S3.

Fluorescence measurement parameters and image process

Fluorescence of FITC (λ_{ex} = 490 nm, λ_{em} = 500–600 nm, laser intensity 100%, gain at 100 for confocal microscope; λ_{ex} = 488 nm, λ_{em} = 505–545 nm for flow cytometry), Cy3 (λ_{ex} = 488 nm, λ_{em} = 564–606 nm for flow cytometry), Hoechst (λ_{ex} = 405 nm, λ_{em} = 410–490 nm, laser intensity 1%, gain at 100 for confocal microscope), and 4-MU (λ_{ex} = 405 nm, λ_{em} = 427.5–472.5 nm for flow cytometry) was collected in respective conditions. In general, 10,000 signals were recorded in a flow cytometer (CytoFLEX) for each sample, and the MFI was calculated based on 3–4 replicates with independently collected pollen from different flowers from random plants with the same genotype growing together (biological replicates) of each sample randomly collected from different flowers. Due to the strong autofluorescence of pollen in 370–600 nm (Supplemental Figure S6A), flow cytometer data within the FITC channel and Cy3 channel (PE channel) were normalized based on the autofluorescence intensity collected from untreated wild-type pollen. The MU fluorescence was normalized based on the average intensity from the untreated GUS-positive pollen for comparison. Confocal microscope images were collected from a Leica SP8 Laser Scanning Confocal Microscopy under a 630× magnification, and pictures were processed with LAS×. Pollen was resuspended in 10 (v/v)% glycerol and dropped onto the slide.

Pollen in vitro germination

Matured pollen grains from random 3–5 fully bloomed tomato flowers were collected with a pollinator. One milliliter of germination media (20 mM MES, pH = 6.0, 3 mM $Ca(NO_3)_2$, 1 mM KCl, 0.8 mM $MgSO_4$, 1.6 mM boric acid, 2.5% (w/v) sucrose, 24% (w/v) PES-4000 [Huang et al., 2014]) containing a certain concentration of LDH nanoparticles was added into a 12-well plate. Pollen grains were carefully poured into germination media without any strong disturbance. Germination was carried out at 27°C in the dark for 3 h. Pollen grains were then collected and observed in a microscope (Zeiss Axioimager 2 fluorescence microscope) with a 10× objective. For each independent treatment, pollen grains (100–270) from nine images collected from different fields of view for each sample were observed, and the tube length was measured. A pollen grain with a tube length of more than twice the pollen grain size was considered as full germination. The statistics data were calculated based on two replicates with pollen grains collected from different flowers for each sample at the LDH-50 nanoparticle concentrations from 50 to 500 mg/L.

Statistical analysis

Data, represented as mean ± standard error of mean (SEM), were analyzed through one-way ANOVA with Bartlett's test to confirm the consistency of deviation, followed by t test for comparison between each group. A $P < 0.05$ was considered statistically significant. In figures with lower case letters above the bars, different letters indicate the statistical difference with $P < 0.05$. For each experiment, biological replicates were conducted with independent treatment and independent collection of pollen (for n times of replicates).

Accession numbers

Sequence data from this article can be found in the GenBank/EMBL data libraries under accession number AJ298139.1.

Supplemental data

The following materials are available in the online version of this article.

Supplemental Figure S1. Correlation between the fluorescence intensity increase and the mass percentage of LDHs.

Supplemental Figure S2. Time-dependent uptake profiles of LDH-30 and LDH-50 nanoparticles at 50 mg/L.

Supplemental Figure S3. Time-dependent fluorescence decay after 2 h uptake of LDH-30-FITC and LDH-50-FITC at 50 mg/L of LDH.

Supplemental Figure S4. Pollen in vitro germination in the presence of LDH-50 nanoparticles.

Supplemental Figure S5. Confocal microscope image analysis of average pixel intensity inside the pollen.

Supplemental Figure S6. Auto-fluorescence of mature pollen grains.

Supplemental Figure S7. Confocal images show the internalization of fluorescein isothiocyanate labeled LDH nanoparticles (LDH-FITC).

Supplemental Figure S8. LDH-50 nanoparticles loading and protection of dsRNA (505 bp).

Supplemental Figure S9. LDH-50 nanoparticle uptake by 1 week-old Arabidopsis root.

Supplemental Table S1. Characteristic parameters of LDH-30, LDH-50, LDH-80, LDH-120 suspension in deionized water and their stability in 2-MES acid (20 mM, pH 6.0) buffer.

Supplemental Dataset S1. Cy3 labeled CMV2b dsRNA sequence.

Supplemental Dataset S2. GUS dsRNA sequence.

Supplemental Dataset S3. Primers for RT-qPCR.

Acknowledgments

Funding

References

Altpeter F, Springer NM, Bartley LE, Blechl AE, Brutnell TP, Citovsky V, Conrad LJ, Gelvin SB, Jackson DP, Kausch AP, et al. (2016) Advancing crop transformation in the era of genome editing. Plant Cell **28**: 1510–1520

Aniento F, Robinson DG (2005) Testing for endocytosis in plants. Protoplasma **226**: 3–11

Avellan A, Yun J, Zhang Y, Spielman-Sun E, Unrine JM, Thieme J, Li J, Lombi E, Bland G, Lowry GV (2019) Nanoparticle size and coating chemistry control foliar uptake pathways, translocation, and leaf-to-rhizosphere transport in wheat. ACS Nano **13**: 5291–5305

Bao W, Wang J, Wang Q, O'Hare D, Wan Y (2016) Layered double hydroxide nanotransporter for molecule delivery to intact plant cells. Sci Rep **6**: 26738

Bates GW (1995) Electroporation of plant protoplasts and tissues. Methods Cell Biol **50**: 363–373

Bohne G, Richter E, Woehlecke H, Ehwald R (2003) Diffusion barriers of tripartite sporopollenin microcapsules prepared from pine pollen. Ann Bot **92**: 289–297

Carroll BJ, Klimyuk VI, Thomas CM, Bishop GJ, Harrison K, Scofield SR, Jones JDG (1995) Germinal transpositions of the maize element dissociation from T-DNA loci in tomato. Genetics **139**: 407–420

Chen W, Zuo H, Li B, Duan C, Rolfe B, Zhang B, Mahony TJ, Xu ZP (2018a) Clay Nanoparticles elicit long-term immune responses by forming biodegradable depots for sustained antigen stimulation. Small **14**: e1704465

Chen W, Zuo H, Zhang E, Li L, Henrich-Noack P, Cooper H, Qian Y, Xu ZP (2018b) Brain targeting delivery facilitated by ligand-functionalized layered double hydroxide nanoparticles. ACS Appl Mater Interfaces **10**: 20326–20333

Cunningham FJ, Goh NS, Demirer GS, Matos JL, Landry MP (2018) Nanoparticle-mediated delivery towards advancing plant genetic engineering. Trends Biotechnol **36**: 882–897

Dan Y, Zhang W, Xue R, Ma X, Stephan C, Shi H (2015) Characterization of gold nanoparticle uptake by tomato plants using enzymatic extraction followed by single-particle inductively coupled plasma-mass spectrometry analysis. Environ Sci Technol **49**: 3007–3014

Demirer GS, Zhang H, Goh NS, Pinals RL, Chang R, Landry MP (2020) Carbon nanocarriers deliver siRNA to intact plant cells for efficient gene knockdown. Science Advances **6**: 12

Demirer GS, Zhang H, Matos JL, Goh NS, Cunningham FJ, Sung Y, Chang R, Aditham AJ, Chio L, Cho MJ, et al. (2019) High aspect ratio nanomaterials enable delivery of functional genetic material without DNA integration in mature plants. Nat Nanotechnol **14**: 456–464

Dong H, Chen M, Rahman S, Parekh HS, Cooper HM, Xu ZP (2014) Engineering small MgAl-layered double hydroxide nanoparticles for enhanced gene delivery. Applied Clay Science **100**: 66–75

Fischer R, Stoger E, Schillberg S, Christou P, Twyman RM (2004) Plant-based production of biopharmaceuticals. Curr Opin Plant Biol **7**: 152–158

Giraldo JP, Landry MP, Faltermeier SM, McNicholas TP, Iverson NM, Boghossian AA, Reuel NF, Hilmer AJ, Sen F, Brew JA, et al.

(2014) Plant nanobionics approach to augment photosynthesis and biochemical sensing. Nat Mater **13**: 400–408

Gu Z, Yan SY, Cheong S, Cao ZB, Zuo HL, Thomas AC, Rolfe BE, Xu ZP (2018) Layered double hydroxide nanoparticles: impact on vascular cells, blood cells and the complement system. J Colloid Interface Sci **512**: 404–410

Hu P, An J, Faulkner MM, Wu H, Li Z, Tian X, Giraldo JP (2020) Nanoparticle charge and size control foliar delivery efficiency to plant cells and organelles. ACS Nano **14**: 7970–7986

Huang WJ, Liu HK, McCormick S, Tang WH (2014) Tomato pistil factor STIG1 promotes in vivo pollen tube growth by binding to phosphatidylinositol 3-phosphate and the extracellular domain of the pollen receptor kinase LePRK2. Plant Cell **26**: 2505–2523

Jiang L, Ding L, He B, Shen J, Xu Z, Yin M, Zhang X (2014) Systemic gene silencing in plants triggered by fluorescent nanoparticle-delivered double-stranded RNA. Nanoscale **6**: 9965–9969

Keddie JS, Carroll BJ, Thomas CM, Reyes MEC, Klimyuk V, Holtan H, Gruissem W, Jones JDG (1998) Transposon tagging of the defective embryo and meristems gene of tomato. Plant Cell **10**: 877–887

Key S, Ma JKC, Drake PMW (2008) Genetically modified plants and human health. J Royal Soc Med **101**: 290–298

Koch A, Kogel KH (2014) New wind in the sails: improving the agronomic value of crop plants through RNAi-mediated gene silencing. Plant Biotechnol J **12**: 821–831

Kurkdjian A, Guern J (1989) Intracellular pH—measurement and importance in cell-activity. Annu Rev Plant Physiol Plant Mol Biol **40**: 271–303

Kwak SY, Lew TTS, Sweeney CJ, Koman VB, Wong MH, Bohmert-Tatarev K, Snell KD, Seo JS, Chua NH, Strano MS (2019) Chloroplast-selective gene delivery and expression in planta using chitosan-complexed single-walled carbon nanotube carriers. Nat Nanotechnol **14**: 447–455

Lew TTS, Park M, Wang YZ, Gordiichuk P, Yeap WC, Rais SKM, Kulaveerasingam H, Strano MS (2020) Nanocarriers for transgene expression in pollen as a plant biotechnology tool. Acs Materials Lett **2**: 1057–1066

Lew TTS, Wong MH, Kwak SY, Sinclair R, Koman VB, Strano MS (2018) Rational Design principles for the transport and subcellular distribution of nanomaterials into plant protoplasts. Small **14**: e1802086

Li B, Gu Z, Kurniawan N, Chen WY, Xu ZP (2017) Manganese-based layered double hydroxide nanoparticles as a T-1-MRI contrast agent with ultrasensitive pH response and high relaxivity. Advanced Materials **29**: 8

Liu J, Nannas NJ, Fu FF, Shi J, Aspinwall B, Parrott WA, Dawe RK (2019) Genome-scale sequence disruption following biolistic transformation in rice and maize. Plant Cell **31**: 368–383

Lv J, Christie P, Zhang S (2019) Uptake, translocation, and transformation of metal-based nanoparticles in plants: recent advances and methodological challenges. Environ Sci Nano **6**: 41–59

Lv ZY, Jiang R, Chen JF, Chen WS (2020) Nanoparticle-mediated gene transformation strategies for plant genetic engineering. Plant J **104**: 880–891

Martin-Ortigosa S, Peterson DJ, Valenstein JS, Lin VS, Trewyn BG, Lyznik LA, Wang K (2014) Mesoporous silica nanoparticle-mediated intracellular cre protein delivery for maize genome editing via loxP site excision. Plant Physiol **164**: 537–547

Martiniere A, Gibrat R, Sentenac H, Dumont X, Gaillard I, Paris N (2018) Uncovering pH at both sides of the root plasma membrane interface using noninvasive imaging. Proc Natl Acad Sci USA **115**: 6488–6493

McLoughlin AG, Wytinck N, Walker PL, Girard IJ, Rashid KY, de Kievit T, Fernando WGD, Whyard S, Belmonte MF (2018) Identification and application of exogenous dsRNA confers plant protection against *Sclerotinia sclerotiorum* and *Botrytis cinerea*. Scientific Rep **8**: 14

Mitter N, Worrall EA, Robinson KE, Li P, Jain RG, Taochy C, Fletcher SJ, Carroll BJ, Lu GQ, Xu ZP (2017) Clay nanosheets for topical delivery of RNAi for sustained protection against plant viruses. Nat Plants **3**: 16207

Oh JM, Choi SJ, Lee GE, Kim JE, Choy JH (2009) Inorganic metal hydroxide nanoparticles for targeted cellular uptake through clathrin-mediated endocytosis. Chem Asian J **4**: 67–73

Patterson AL (1939) The Scherrer formula for X-ray particle size determination. Phys Rev **56**: 978–982

Polowick PL, Sawhney VK (1993a) An ultrastructural-study of pollen development in tomato (*Lycopersicon esculentum*).1. Tetrad to early binucleate microscpore stage. Can J Bot **71**: 1039–1047

Polowick PL, Sawhney VK (1993b) An ultrastructural-study of pollen development in tomato (Lycopersicon-esculentum).2. Pollen maturation. Can J Bot **71**: 1048–1055

Reynolds GD, Wang C, Pan J, Bednarek SY (2018) Inroads into internalization: five years of endocytic exploration. Plant Physiol **176**: 208–218

Sadeghi R, Rodriguez RJ, Yao Y, Kokini JL (2017) Advances in nanotechnology as they pertain to food and agriculture: benefits and risks. Annu Rev Food Sci Technol **8**: 467–492

Schwab F, Zhai G, Kern M, Turner A, Schnoor JL, Wiesner MR (2016) Barriers, pathways and processes for uptake, translocation and accumulation of nanomaterials in plants–Critical review. Nanotoxicology **10**: 257–278

Shivanna KR, Heslopharrison J (1981) Membrane state and pollen viability. Annals of Botany **47**: 759–770

Sun XD, Yuan XZ, Jia YB, Feng LJ, Zhu FP, Dong SS, Liu JJ, Kong XP, Tian HY, Duan JL, et al. (2020) Differentially charged nanoplastics demonstrate distinct accumulation in *Arabidopsis thaliana*. Nat Nanotechnol **15**: 755–760

Wang H, Jiang L (2011) Transient expression and analysis of fluorescent reporter proteins in plant pollen tubes. Nat Protoc **6**: 419–426

Wang P, Lombi E, Zhao FJ, Kopittke PM (2016) Nanotechnology: a new opportunity in plant sciences. Trends Plant Sci **21**: 699–712

Wang QL, Kong LG, Hao HQ, Wang XH, Lin JX, Samaj J, Baluska F (2005) Effects of brefeldin A on pollen germination and tube growth. Antagonistic effects on endocytosis and secretion. Plant Physiol **139**: 1692–1703

Wong MH, Misra RP, Giraldo JP, Kwak SY, Son Y, Landry MP, Swan JW, Blankschtein D, Strano MS (2016) Lipid exchange envelope penetration (LEEP) of nanoparticles for plant engineering: a universal localization mechanism. Nano Lett **16**:1167–1172.

Xu ZP, Niebert M, Porazik K, Walker TL, Cooper HM, Middelberg APJ, Gray PP, Bartlett PF, Lu GQ (2008) Subcellular compartment targeting of layered double hydroxide nanoparticles. J Control Rel **130**: 86–94

Xu ZP, Stevenson GS, Lu CQ, Lu GQM, Bartlett PF, Gray PP (2006a) Stable suspension of layered double hydroxide nanoparticles in aqueous solution. J Am Chem Soc **128**: 36–37

Xu ZP, Walker TL, Liu KL, Cooper HM, Lu GQM, Bartlett PF (2007) Layered double hydroxide nanoparticles as cellular delivery vectors of supercoiled plasmid DNA. Int J Nanomed **2**: 163–174

Xu ZP, Zeng HC (2001) Abrupt structural transformation in hydrotalcite-like compounds Mg1-xAlx(OH)(2)(NO3)(x)center dot nH(2)O as a continuous function of nitrate anions. J Phys Chem B **105**: 1743–1749

Xu ZP, Zeng QH, Lu GQ, Yu AB (2006b) Inorganic nanoparticles as carriers for efficient cellular delivery. Chem Eng Sci **61**: 1027–1040

Zhang H, Demirer GS, Zhang H, Ye T, Goh NS, Aditham AJ, Cunningham FJ, Fan C, Landry MP (2019) DNA nanostructures coordinate gene silencing in mature plants. Proc Natl Acad Sci U S A **116**: 7543–7548

Zhang LX, Hu J, Jia YB, Liu RT, Cai T, Xu ZP (2021) Two-dimensional layered double hydroxide nanoadjuvant: recent progress and future direction. Nanoscale **13**: 7533–7549

Zhao X, Meng Z, Wang Y, Chen W, Sun C, Cui B, Cui J, Yu M, Zeng Z, Guo S, et al. (2017) Pollen magnetofection for genetic modification with magnetic nanoparticles as gene carriers. Nat Plants **3**: 956–964